ELSEVIER

Chemical Engineering Journal 136 (2008) 210–220

Chemical Engineering Journal

www.elsevier.com/locate/cej

Microfiltration of water in oil emulsions and evaluation of fouling mechanism

B. Hu [a], K. Scott [b,*]

[a] *Department of Chemical Engineering, University of Birmingham, Edgbaston, Birmingham B15 2TT, UK*
[b] *School of Chemical Engineering and Advanced Materials, University of Newcastle upon Tyne University of Newcastle, Merz Court, Newcastle upon Tyne NE1 7RU, UK*

Received 12 May 2006; received in revised form 25 March 2007; accepted 1 April 2007

Abstract

An analysis of the crossflow microfiltration of water in oil emulsions is reported. The emulsion considered was water, containing copper sulphate with kerosene using Span 80 as surfactant. Three membrane materials were studied: PTFE, PVDF and regenerated cellulose. The effects of crossflow velocity, transmembrane pressure, and temperature are analysed using several cake filtration models. Increases in transmembrane pressure, temperature and flow rate of emulsion all result in an increase in membrane flux. Membrane flux declines initially with time under most conditions of operation, except at a temperature of 50 °C, where values of flux are stable. Analysis of the fall in flux with time for the PTFE and PVDF membranes indicates that cake formation gives the best prediction of behaviour. In the case of PVDF the model does not predict the performance over the complete range of filtration times but rather two stages of filtration appear to occur; possibly cake formation initially followed by some intermediate pore blocking. In the case of the regenerated cellulose membrane, two stages of filtration seem to occur: an initial phase of cake formation or some pore blocking followed by intermediate pore blocking.

Keywords: Membrane; Crossflow filtration; Microfiltration; Emulsions; Filtration models

1. Introduction

Separation of water from water in oil emulsions is of importance in several industries, e.g. organic solvent and vegetable oil, for the recovery of solvents and the purification of oil. The standard method for the treatment of emulsions is chemical demulsification followed by gravity settling. This process requires the use of a variety of chemicals and the water phase from chemical treatment needs secondary purification. This will therefore entail additional energy requirements and hence higher cost.

Several effective methods have been recently developed for oil–water emulsion separation such as coalescence of dispersion in fibrous beds, biodegradation and biotransformation of oily wastes, and application of electric field to coalesce droplets. The development of membrane technologies has most recently embodied applications in the processing of emulsions. Several studies have reported that crossflow membrane microfiltration (CFMF) (and ultrafiltration) are effective processes in concentrating oil–water emulsions [1–7]. Many different approaches can be used to improve the flux in CFMF of emulsions.

CFMF requires relatively low transmembrane pressures (<0.35 MPa). The typical flux rates with clean membranes are between 10^{-4} m s^{-1} and 10^{-2} m s^{-1} which are much higher than in UF and reverse osmosis. In crossflow microfiltration (CFMF), based on surface filtration the fluid suspension flows parallel to the membrane and the imposed transmembrane pressure drop causes permeation flow through the microporous membrane and thus only a thin cake layer forms. This method is an effective way to control the "cake" build up and thus a relatively high flux rate can be maintained over a prolong period of time.

Due to relatively modest operation requirement, flexibility and higher membrane performance of CFMF, the technique has found a wide range of applications. Although, there are numerous applications of crossflow filtration, only a few are related to the separation of water/oil emulsions. Anderson et al. [8] effectively separated oil from water emulsion. Their experimental results showed that crossflow filtration is feasible for the concentration of oily waste by using ultrafiltration. Le Barre and Daufan [9] demonstrated separation of casein micelles from whey proteins through CFMF of skimmed milk with a ceramic membrane.

* Corresponding author. Tel.: +44 191 222 8771; fax: +44 191 222 5292.
E-mail addresses: k.scott@ncl.ac.uk, K.Scott@newcastle.ac.uk (K. Scott).

1385-8947/$ – see front matter © 2007 Elsevier B.V. All rights reserved.
doi:10.1016/j.cej.2007.04.003

There are several reports on separation of oil/solvent in water emulsions [5,10–12]. Lee et al. [13] used a ceramic membrane for the crossflow microfiltration of soluble waste oil. This membrane was tested with a soluble waste oil which consisted of oil droplets whose mean diameter was 11 μm. The effects of the velocity and backflushing time on permeate flux were investigated. Limayem et al. [14] have considered the purification of nanoparticle suspensions by a concentration/diafiltration process. Ripperger [15] has recently reviewed the state of the art in crossflow microfiltration. The information obtained in the above system may not be suitable in water in oil emulsion system especially when the interaction of membrane and droplet maybe important.

This paper reports data for the crossflow microfiltration of water in oil emulsions, using kerosene as the organic phase. The performance, i.e. the change in flux rate with time is analysed using several "cake" filtration models to determine the most appropriate applicable to microfiltration of water in oil emulsions for specific membrane materials.

2. Experimental

2.1. Membranes

The membranes used in this work were:

- PTFE, Schleicher & Schuell (S&S), hydrophobic, 151 μm thickness, 0.2 μm pore size.
- PTFE, Gore-Tex®, hydrophobic, 185 μm thickness, 0.2 μm pore size.
- PVDF, Schleicher & Schuell (S&S), hydrophobic, 132 μm thickness, 0.2 μm pore size.
- Regenerated cellulose Schleicher & Schuell (S&S), hydrophilic, 118 μm thickness, 0.15 μm pore size.

2.2. Emulsion characteristics

The method of Dean and Stark was used to determine the water content of the emulsion. During this test the sample is heated under reflux with an organic liquid (toluene) which is immiscible with water. The water and toluene are boiled off and reflux from the condenser is collected in a graduated vessel below the condenser. The water separates below the toluene and its volume may be measured directly. Water content greater than 2000 ppm can be detected with this method.

The dynamic viscosity of the emulsion was determined using an Oswald viscometer. The kinematic viscosity of the emulsion and oil solution in various compositions was determined by a Redwood viscometer. The correlation between viscosity and temperature were also determined by the Redwood viscometer by varying the temperature of water in the jacket.

The emulsion density was measured using a Westphal Balance which has been widely applied for petroleum oil measurement, and is especially suitable for viscous fluids or two-phase liquid mixtures.

2.3. Emulsion formulation

The original water in oil emulsions were prepared by adding an aqueous phase to the oil phase, and stirring for 15 min at 5500 rpm (measured by a Flush Strobe). The oil phase was made by adding surfactant Span 80 (Sorbitan Monooleate, generally, of about 3% by weight) to the kerosene. The aqueous phase was made by adding 2% (by weight) cupric sulphate to the purified de-ionised water produced by a Millipore water purification system. The cupric sulphate solution here was used as an indicator to facilitate determination of the degree of fouling on the membrane surface and to simulate a metal extraction system. To make emulsions with various concentrations, the concentrated emulsion was dispersed into kerosene containing the same amount of surfactant.

Preparation of emulsions by mixing was accomplished using a single stage stirrer, using one of four different types of blades (two with sharp knife, two with gear), powered by a Citenco Model BS 5000 motor (Park Products Ltd.). The allowed maximum rpm was 6000. A PTFE disc with a hole of 15 mm diameter was placed on the top of the beaker to prevent the spillage of emulsion during agitation.

2.4. The membrane module

The membrane module shown in Fig. 1, was composed of two pieces of machined circular polypropylene. The upper section contains a rectangular channel (25 mm × 66 mm) with a 3 mm deep recess for emulsion flow. The base section includes a rectangular section (38 mm × 79 mm) which supports the membrane for the removal of permeate which has three 1 mm holes for drainage of permeate. The membrane sheet with effective area 16.5 cm^2 is wetted by pure kerosene to prevent the surfactant adsorbing on the membrane surface, then placed on a permeate mesh spacer (same dimensions as the membrane sheet) which is mounted on the recess in the base section then sealed with the O-ring gaskets. The membrane module unit is secured with six tie bolts. The emulsion flows parallel along the membrane surface. The filtrate (containing kerosene and Span 80 if the separation rate is 100%) flows tangentially out through the membrane to the collection chamber.

2.5. Crossflow microfiltration rig

The experimental rig for crossflow microfiltration is shown in Fig. 2. The emulsion was delivered from the feed tank, fitted with a water jacket for temperature control, by means of a centrifugal recirculation pump into the membrane unit. The flow rate of fluid was adjusted by varying the revolutions of the gear pump and was measured by the rotameter. The rotameter was calibrated using a 30% (wt/wt) emulsion. Two pressure gauges, fitted at the inlet and outlet of the membrane unit, are used to monitor system transmembrane pressure. The transmembrane pressure was adjusted by regulating a valve which can exert a backpressure along the membrane unit. As the outlet for permeation was open to the air, the average value of the two pressure meters is assumed to be the transmembrane pressure. Filtrate

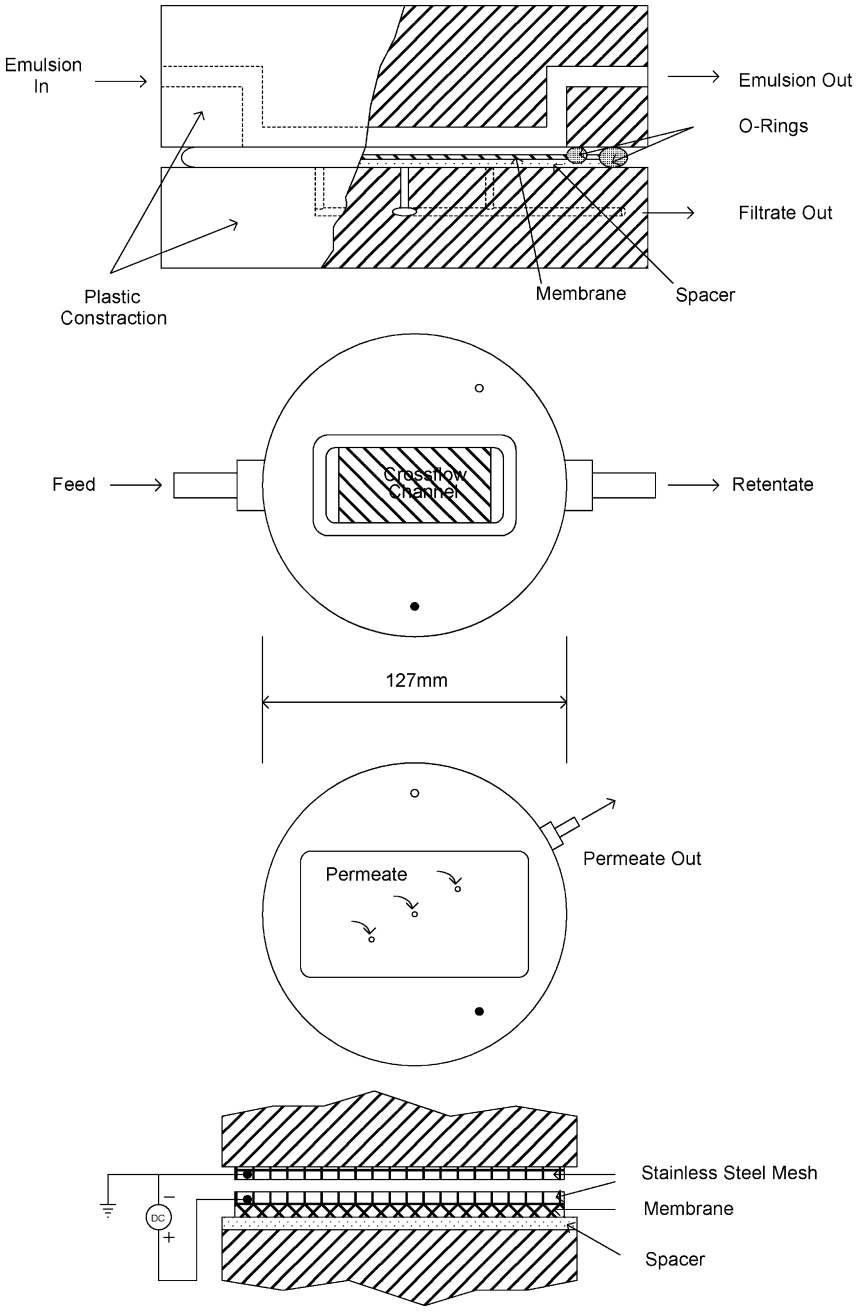

Fig. 1. Schematic diagram of membrane module unit. (a) Side sectional view. (b) Top and base sections of module. (c) Module with electrode connected.

was collected in the filtrate receiver and is manually added to the feed tank to maintain the water concentration of the emulsion constant. The permeate rate was monitored by means of an electric balance (supplied by Denver Instrument Company) connected to a PC. The balance was model 4 K with capacity of 4000 g and resolution of 0.01 g. Data was recorded at 15–60 s intervals depending on the flux rate and graphically displayed on the screen of the PC. The retentate was continually recycled to the feed vessel (using a stirrer at an agitation speed of 200 rpm), where it was mixed with the emulsion.

Each experimental run used approximately 1.2 dm^3 of freshly prepared emulsion. For determination of the effect of temperature on the membrane filtration, the emulsion was first heated to the run temperature before starting the filtration. Once the desired temperature was achieved the emulsion was recycled through the unit until the transmembrane pressure drop is stable. The permeate collection was then started at this point.

To prevent residual emulsion in the system blocking the pipe work which may cause measurement error or even damage of the pipe work due to the corrosion by kerosene, a cleaning system is used. Immediately after each set of tests, the emulsion is completely drained from the system. The following cleaning procedure was then adopted.

(i) the unit was flushed with 6 dm^3 of used kerosene permeate containing small amounts of surfactant which

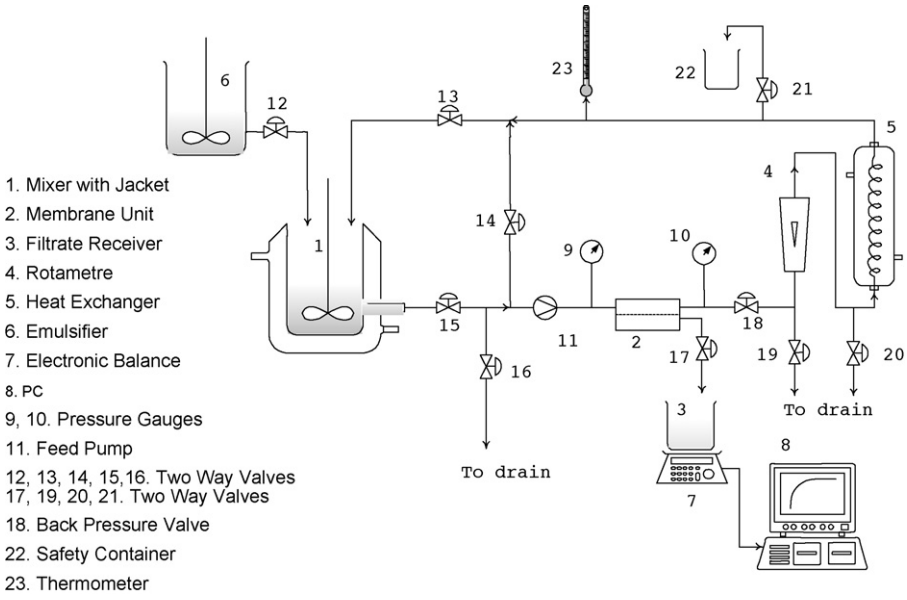

Fig. 2. Crossflow microfiltration diagram.

more easily absorb the emulsion remaining in the system.

(ii) recycle 2 dm^3 of kerosene until both permeate and retentate was clear and then drain the unit.

(iii) recycle pure distilled kerosene for about 30 min or until pure clear kerosene was observed when it is recycled back to the feed tank.

(iv) drain the unit and repeat the procedure. Finally measure the pure kerosene permeate flow rate, to evaluate the cleaning, until the initial flux was obtained.

3. Fouling cake filtration models

The ability of a simple cake filtration analysis to predict the variation in fluxrate with time during crossflow filtration has led to various fouling mechanisms to be proposed to better characterise the flux performance. The various fouling mechanisms that have widely used are cake filtration, intermediate law, standard pore blocking and complete pore blocking [16]. By combining various developments on the filtration models [17,2], the various correlations in each mechanism and reformulated in terms of flux per unit time as follows:

a. Complete pore blocking

$$J = J_0 \, e^{-k_b t} \tag{1}$$

b. Gradual pore blocking (or sometimes called standard pore blocking)

$$J = J_0 \left(1 + \tfrac{1}{2} K_s (A J_0)^{0.5} t\right)^{-2} \tag{2}$$

c. Intermediate filtration

$$J = J_0 (1 + K_i A J_0 t)^{-1} \tag{3}$$

d. Cake filtration

$$J = J_0 (1 + 2K_0 (A J_0)^2 t)^{-0.5} \tag{4}$$

where J_0 depends on the transmembrane pressure, membrane resistance and viscosity of the filtrate and is expressed as $J_0 = \Delta P / \mu R_m$. The various K terms represent mass transfer coefficients for the associated filtration laws.

In the case of constant pressure filtration, the term AJ_0 is constant and the filtration laws can be simplified to:

a. Complete pore blocking

$$\ln(J^{-1}) = \ln(J_0^{-1}) + k_b t \tag{5}$$

b. Gradual pore blocking (or sometimes called standard pore blocking)

$$J^{-0.5} = J_0^{-0.5} + k_s t \tag{6}$$

c. Intermediate filtration

$$J^{-1} = J_0^{-1} + k_i t \tag{7}$$

d. Cake filtration

$$J^{-2} - J_0^{-2} + k_c t \tag{8}$$

where $k_s = (1/2) K_s A^{1/2}$, $k_i = K_i A$, $k_c = 2K_c A^2$.

Consequently plotting the left-hand side flux functions for each model against time are the tests to determine the more appropriate model and the means to obtain the mass transport parameters from the slope.

The analysis considers several membrane materials and investigates both low and high transmembrane pressures.

4. Effect of operating parameters on microfiltration

4.1. Effect of crossflow velocity

Fig. 3 shows typical variation in flux with time for a PTFE membrane. The effect of an increase in crossflow velocity (U_c) on membrane flux performance is clearly seen to improve flux rate.

For crossflow filtration of water in oil emulsion (w/o), because of the possibility of droplets deformation and interactions, the effect of crossflow velocity may or may not be the same as in the typical microfiltration processes mentioned above.

For the emulsion system, factors such as viscosity and density can greatly affect the flux performance, thus the correlation of the flux and Reynolds Number (which is a function of viscosity and density) is valuable in describing the membrane flux performance at various flow conditions. From Fig. 4 the correlation of flux with Reynolds Number is

$$J = K\,Re^n \tag{9}$$

where K is a constant which is equal to 2.87×10^{-2} $dm^3\,m^{-2}\,s^{-1}$, and the exponent n is equal to 0.9 for the high crossflow velocities used.

Overall, crossflow velocity has a marked effect on membrane flux performance when the pressure drop, in the channel is small.

4.2. Cake filtration analysis

The filtration models in Section 3 were tested using three membrane, PTFE, PVDF and regenerated cellulose. Fig. 5 shows the correlation of the models for a PTFE membrane at 400 kPa transmembrane pressure. In most cases the models exhibit a reasonable agreement with experimental data giving linear correlations. The model correlations for each case are given in

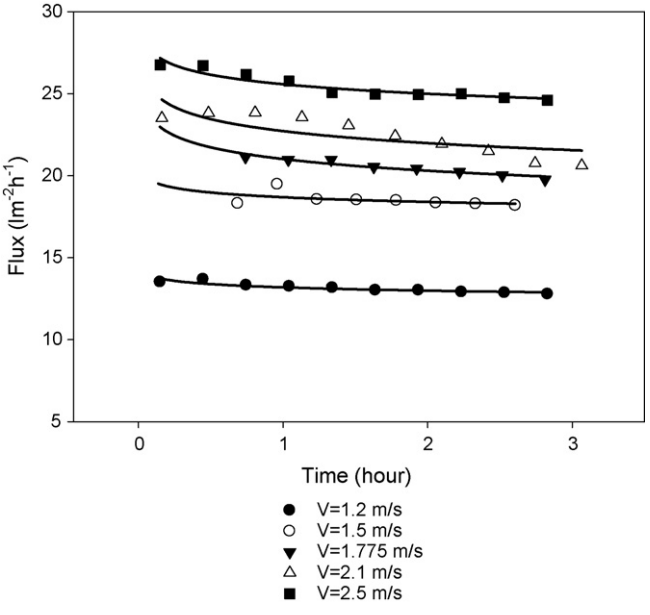

Fig. 3. The permeate flux as a function of time. Membrane: Gore-Tex, 0.2 μm; P_{tm}: 0.6 bar; temperature: 25 °C.

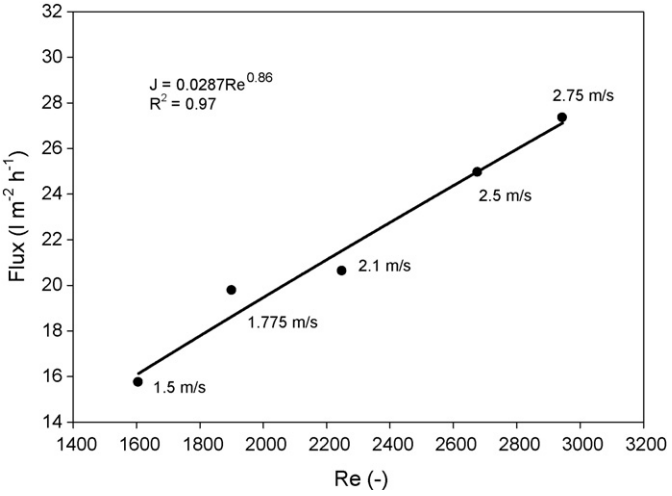

Fig. 4. Steady state flux variation at high crossflow velocity with PTFE membrane.

Fig. 5. The estimation of the flux at $t = 0$ (J_0), from the intercept, gives the following values, 1.077, 1.064, 1.058 and 1.054 cm h^{-1} for the cake filtration, intermediate pore blocking, standard pore blocking and complete pore blocking models, respectively. These values are less than the initial experimental flux, measure at 1.10 cm h^{-1} (from the first data point). Thus each model tends to underestimate the initial flux, as indicated in the lack of correlation at the initial time period of filtration. Using the model correlations for each case considered a comparison is made (Fig. 6) with the experimental data. The best agreement with experimental data is given by the cake formation model which tends to agree with the fouling behaviour observed in traditional solids filtration [18].

The performance data for the PVDF membrane was analysed in the same way as for the PTFE membrane. As Fig. 7 shows, the behaviour of PVDF is quite different to that of PTFE. In this case there is not a single linear correlation of the data over the complete range of filtration times. There appears to be two

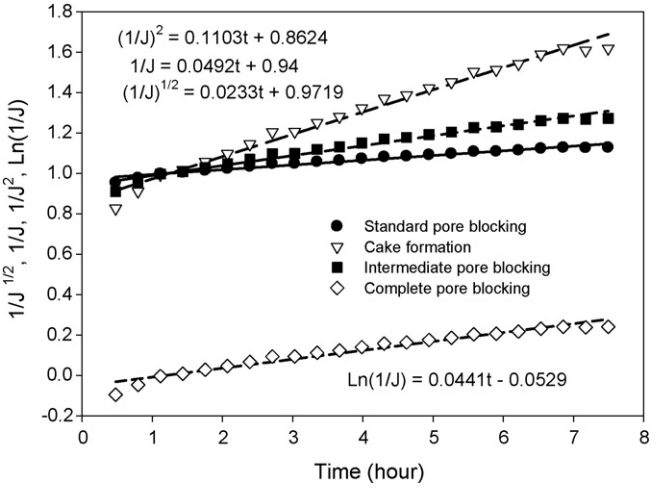

Fig. 5. Variation of flux functions with time for the four filtration models. Membrane 0.2 μm PTFE Schleicher & Schuell, transmembrane pressure 30 kPa, 1.3 m s^{-1}, $T = 30$ °C, emulsion content 30%.

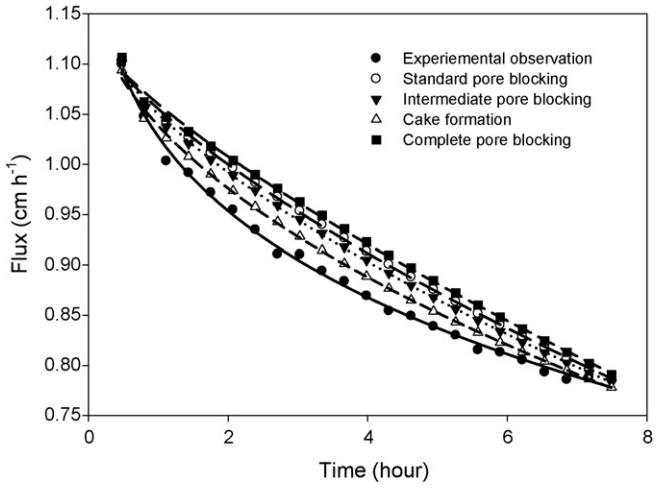

Fig. 6. Comparison of filtration model prediction with experimental data for PTFE. Conditions as in Fig. 5.

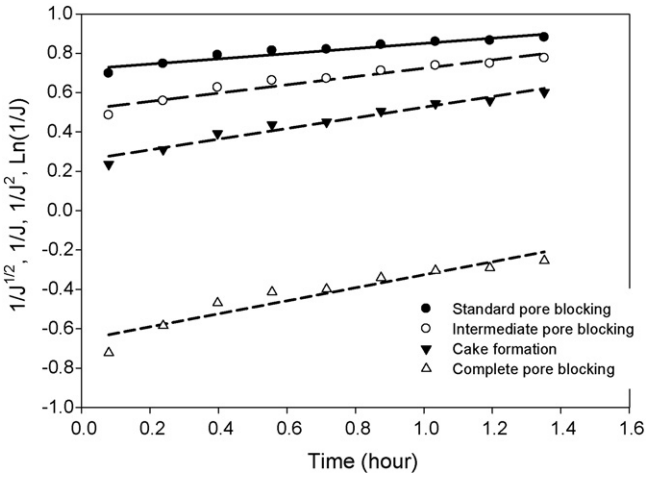

Fig. 8. Variation of flux functions with time for the four filtration models at times less than 1.5 h. Membrane PVDF Schleicher & Schuell, transmembrane pressure 30 kPa, 1.3 m s^{-1}, T = 30 °C, emulsion content 30%.

filtration regions; one at less than 1.5 h and the other >1.5 h. Thus according to the models high mass transport rates occur at the initial filtration times and lower mass transport rates occur at the longer filtration times.

Membrane PVDF Schleicher & Schuell, transmembrane pressure 30 kPa, 1.3 m s^{-1}, T = 30 °C, emulsion content 30% (wt/wt).

The experimental data was thus analysed separately in the two time ranges. Fig. 8 shows the linear correlations of the various models in the low filtration time range, where reasonable correlations are achieved (as shown in the figure). The ability of the resulting model correlations to predict filtration flux with time as shown in Fig. 9 is poor in all cases except perhaps for the cake formation law.

The correlation of the filtration laws at times >1.5 h is shown in Fig. 10. In the case of all models a reasonable correlation exists and this is reflected in the ability of the models to predict the variation of filtration flux with time as shown in Fig. 11.

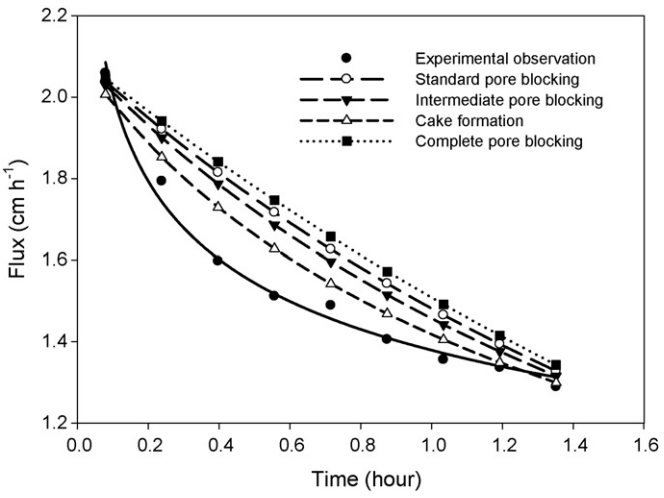

Fig. 9. Comparison of filtration model prediction with experimental data for PVDF. Conditions as in Fig. 8.

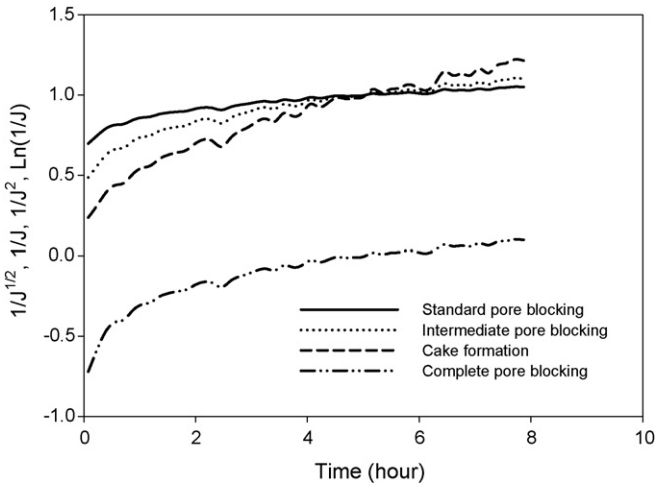

Fig. 7. Variation of flux functions with time for the four filtration models. Membrane PVDF Schleicher & Schuell, transmembrane pressure 30 kPa, 1.3 m s^{-1}, T = 30 °C, emulsion content 30%.

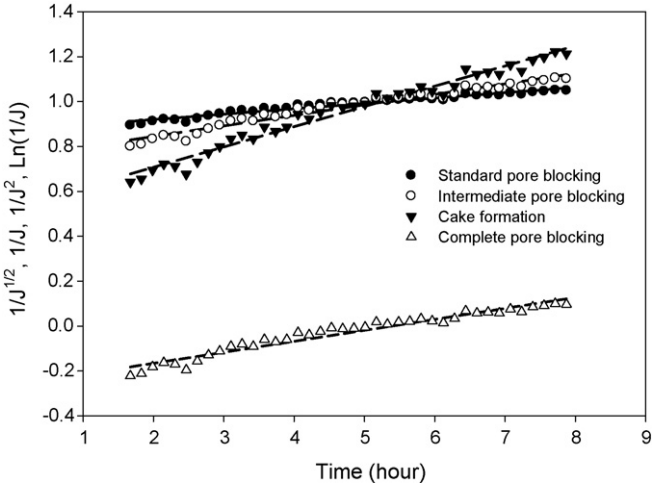

Fig. 10. Variation of flux functions with time for the four filtration models at times greater than 1.5 h. Membrane PVDF Schleicher & Schuell, transmembrane pressure 30 kPa, 1.3 m s^{-1}, T = 30 °C, emulsion content 30%.

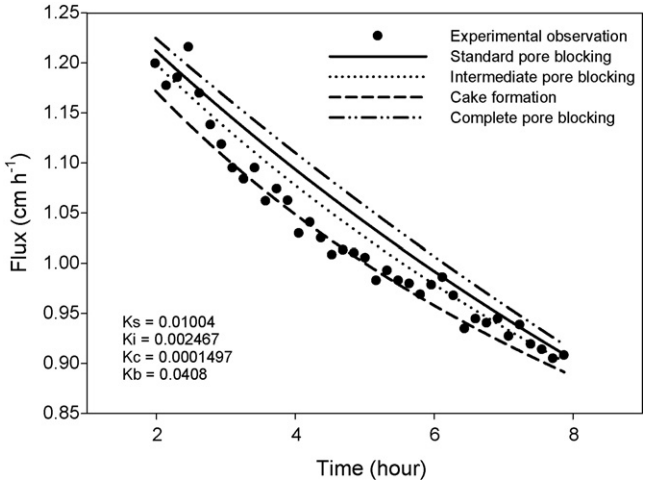

Fig. 11. Comparison of filtration model prediction with experimental data for PVDF. Conditions as in Fig. 10.

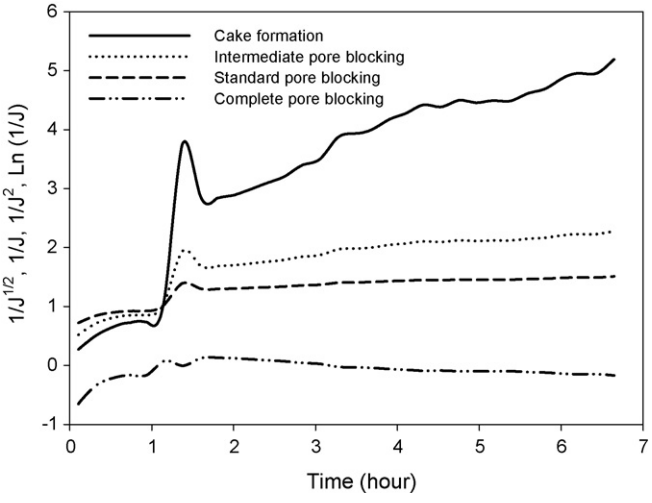

Fig. 12. Variation of flux functions with time for the four filtration models. Membrane regenerated cellulose. 0.15 μm, transmembrane pressure 30 kPa, 1.3 m s^{-1}, T = 30 °C, emulsion content 30%.

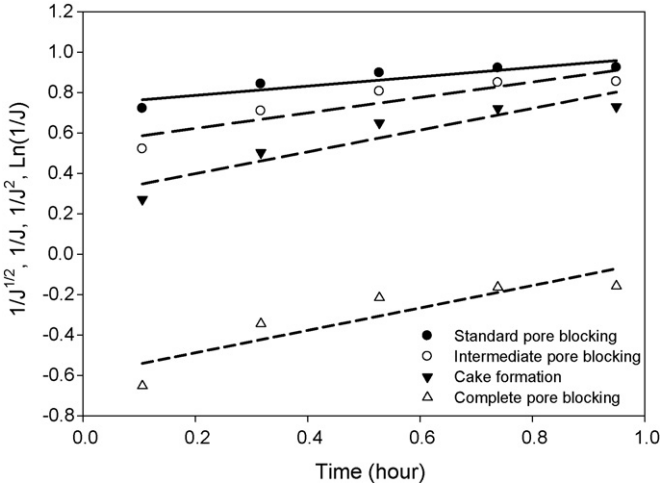

Fig. 13. Variation of flux functions with time for the four filtration models at times less than 1.5 h. Membrane regenerated cellulose, transmembrane pressure 30 kPa, 1.3 m s^{-1}, T = 30 °C, emulsion content 30%.

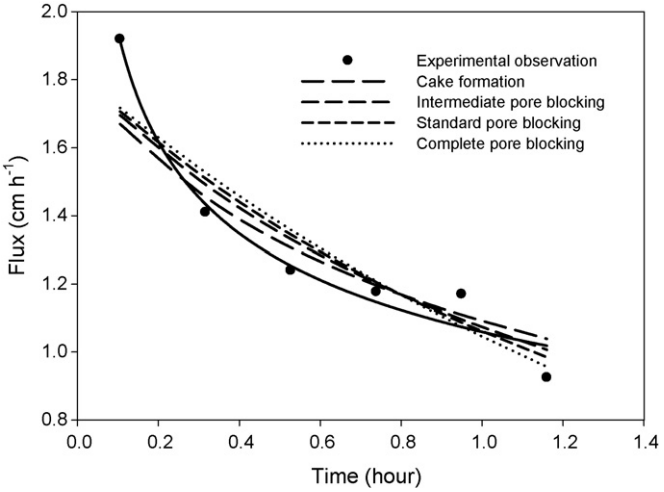

Fig. 14. Comparison of filtration model prediction with experimental data. Conditions as in Fig. 13.

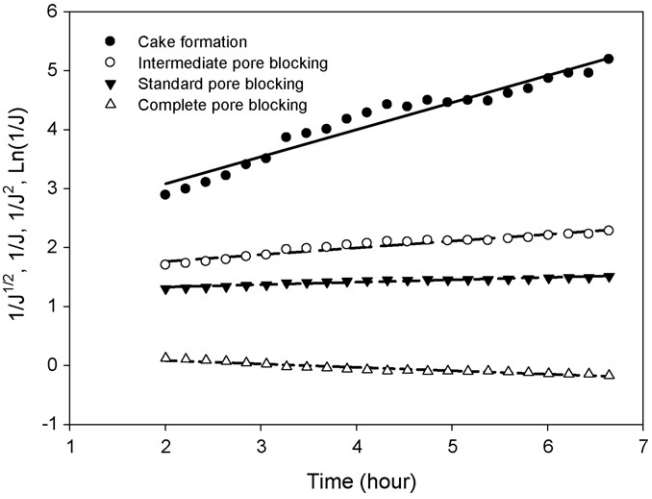

Fig. 15. Variation of flux functions with time for the four filtration models at times greater than 1.5 h. Membrane regenerated cellulose, transmembrane pressure 30 kPa, 1.3 m s^{-1}, T = 30 °C, emulsion content 30%.

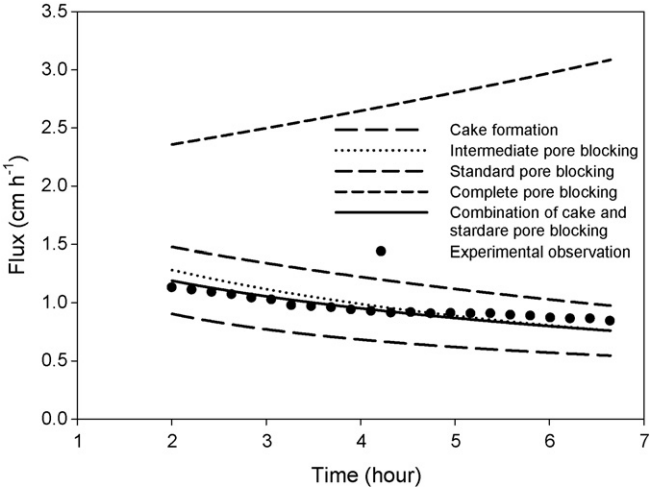

Fig. 16. Comparison of filtration model prediction with experimental data. Conditions as in Fig. 15.

The best prediction of filtration flux is achieved with the cake formation law. Overall it appears that in the case of PVDF the cake formation model gives the best predictions of flux.

Fig. 12 shows the correlations for the four filtration models for the case of the hydrophilic regenerated cellulose membrane. Clearly no model gives a good correlation over the complete range of filtration times and roughly two regions of filtration appear to occur. Consequently model correlations were attempted in both regions; at short and long filtration times.

Figs. 13 and 14 show the correlation of the models and the predictions of the flux performance of the models at short filtration times for the hydrophilic membrane. All the models at the initial stage of filtration underestimate the filtration rates. This may be attributed to the membrane itself which exhibits a high resistance due to its hydrophilic properties, when the emulsion first contact the membrane surface.

The analysis of the data using the models for the longer filtration times is shown in Fig. 15. The corresponding predictions of flux; from the model correlations are shown in Fig. 16. As can be seen in Fig. 16 the complete pore blocking model is not appropriate. The intermediate pore blocking model appears to give the better correlation of the data. This situation would correspond to the behaviour of the emulsion filtration with the hydrophilic membrane where the emulsion passed through the membrane due to the relatively high pressure used. The standard pore blocking and cake formation over and under predict

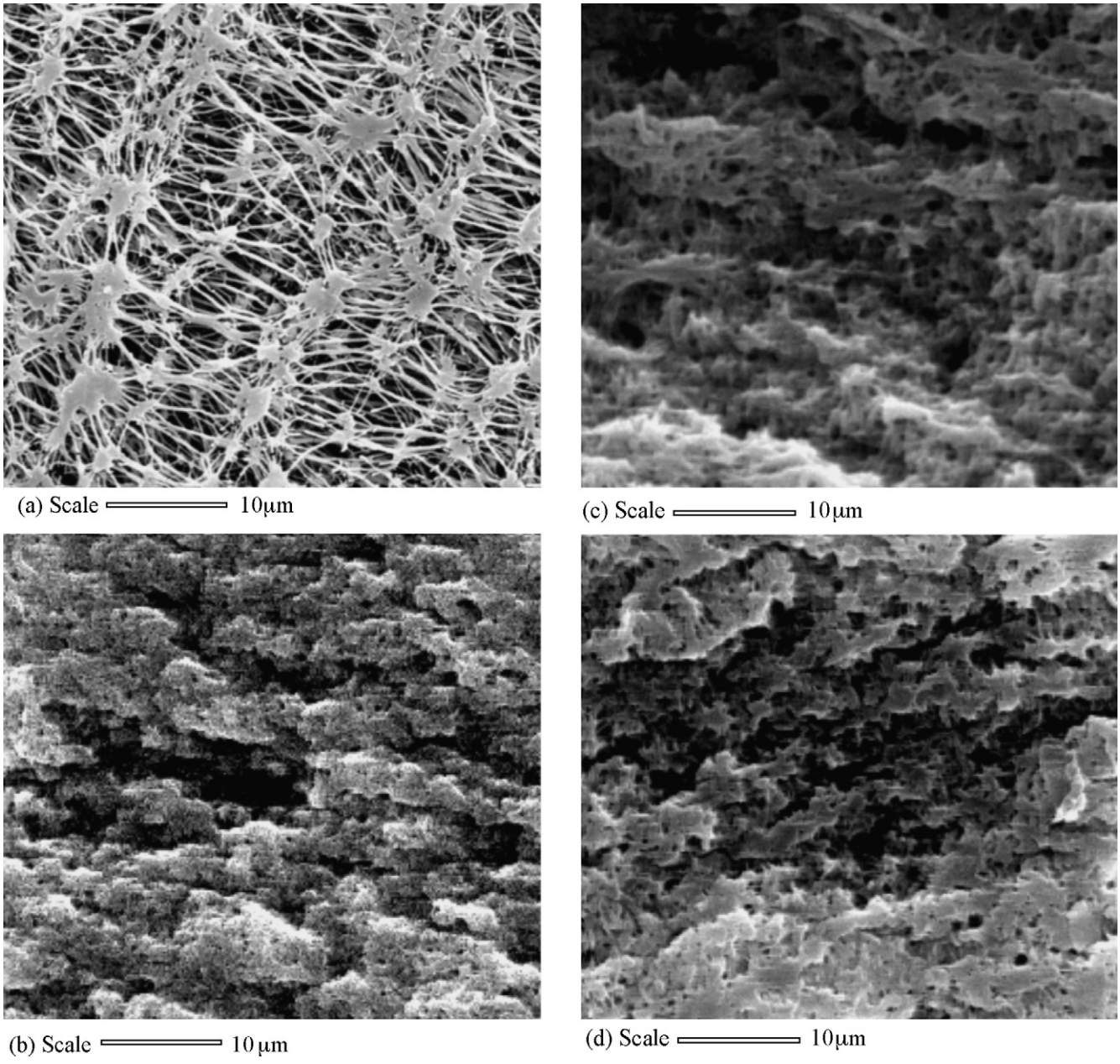

Fig. 17. SEM of new and used PTFE membranes. (a) New, (b) low crossflow velocity, (c) high crossflow velocity, (d) high pressure difference, and (e) cleaned membrane (conditions as in Table 1).

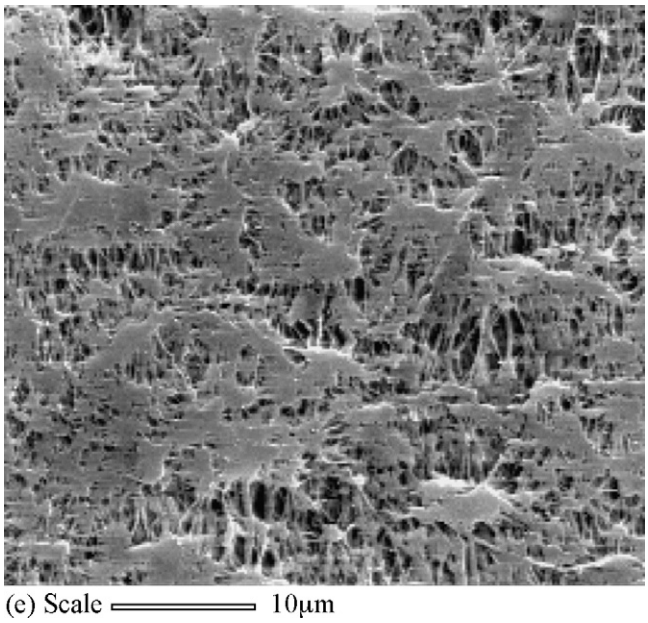

Fig. 17. (*Continued*).

the flux performance, respectively. However, the best agreement between model and experimental flux is actually achieved by averaging the performance of the latter two models as shown in Fig. 16.

4.3. Fouling analysis of the membrane surface

To estimate the effect of emulsion filtration on the surface of the membrane and the accumulation of any "fouling" layer SEM and energy dispersive X-ray analysis (EDAX) was carried out. To enable the extent of surface fouling to be determined 2% $CuSO_4$ was used as an indicator in the water phase. Thus by analysing the copper deposited on the membrane enabled a quantitative estimation of fouling to be determined. Figs. 17 and 18 show the SEM of the new and used membrane surface for Gore PTFE and S&S PTFE, respectively. Table 1 shows the measured extent of fouling as determined from the amount of copper deposited for various conditions of velocity and pressure for the Gore PTFE membrane. The extent of fouling were 5.2%, 1.27% and 2.28% for low crossflow velocity, high crossflow velocity and high transmembrane pressure, respectively.

The SEM of the membrane surfaces generally show that the extent of fouling of the membrane is much greater at low crossflow velocities (Fig. 17b) than at higher crossflow velocities (Fig. 17c) where less coverage of the surface by foulant occurs.

Table 1
Membrane surface coverage measured by SEM

Test sample (used PTFE membrane)	Element (Cu) area percentage in SEM measuring area (%)
G1*	5.2
G2*	1.27
G3*	2.28

Increasing the filtration pressure had the effect of increasing the amount of foulant deposited on the surface. The fouling of the membrane during filtration was not reversible as attempts to clean the membrane using acetone and water and backflushing did not remove all the surface deposit as shown in Fig. 17e.

4.4. Effect of temperature

Temperature is a factor, expected to significantly affect the emulsion system especially in the presence of surfactant. The typical effect of temperature on flux is illustrated in Fig. 19. The crossflow velocity was maintained at $1.3\,m\,s^{-1}$. There was a decline from the initial flux, $16.9\,dm^3\,m^{-2}\,h^{-1}$ down to $12\,dm^3\,m^{-2}\,h^{-1}$ at the temperature, of 25 °C. The flux decline of approximately 32% could be attributed to the lower mass transfer rate, at the low temperature, when the emulsion droplets may easily accumulate on the membrane surface. As the temperature increased, the degree of flux decline was smaller. The filtration performed at 55 °C over seven hours, shows a near constant flux. There are several factors that may cause the increase in flux with increase in temperature.

i. The fouling dynamic resistance R_i and R_f, are strongly temperature dependent.
ii. The average channel Reynolds number increases as the viscosity of the emulsion decreases at a higher temperature resulting in an increase in turbulence in the channel.
iii. The decrease in emulsion viscosity due to increase in temperature may also influence the phase behaviour of the emulsions deposited on the membrane surface. This can be demonstrated by measuring the droplet size of the emulsions after CFMF. The increase of droplets size at higher temperatures may reduce the opportunity for droplets to plug the

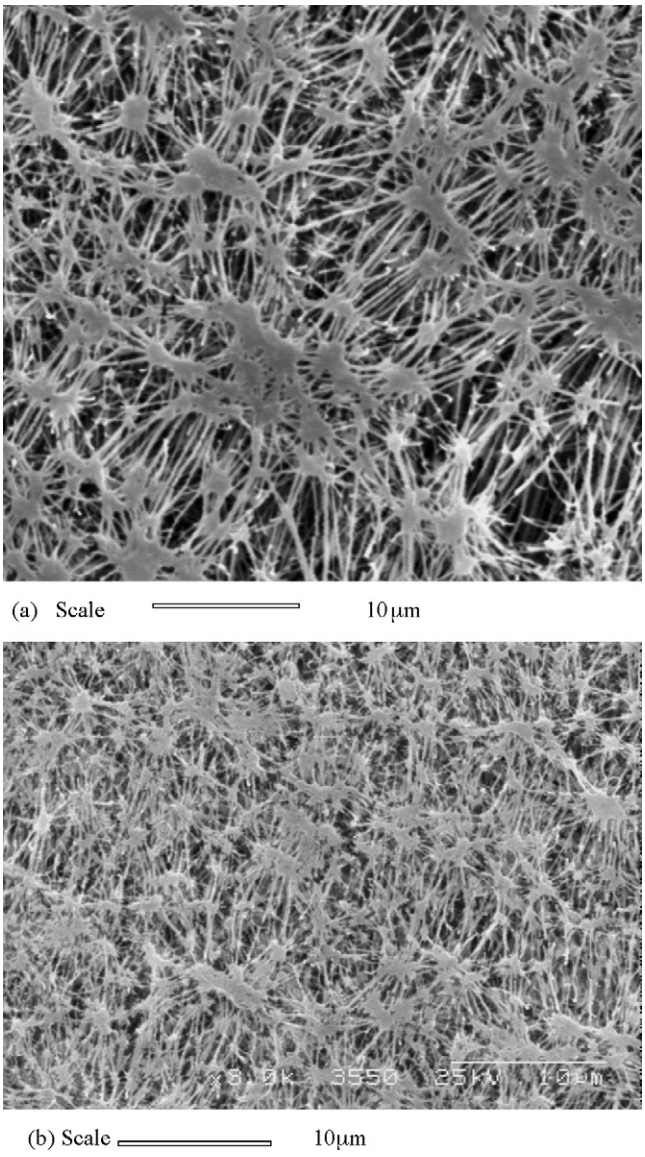

Fig. 18. SEM of new and used PTFE membranes. (a) New and (b) used.

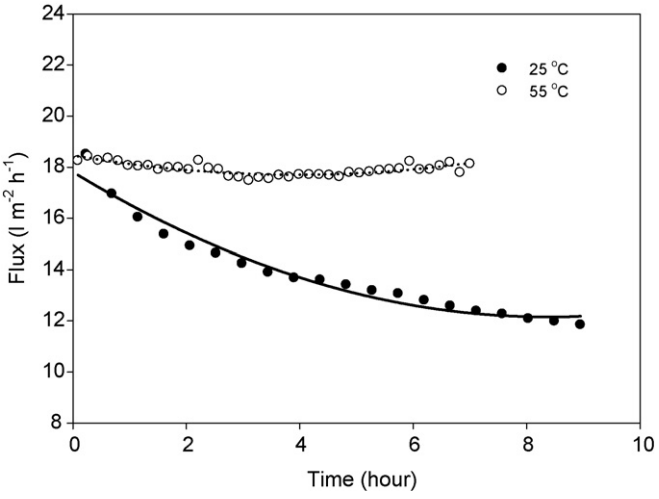

Fig. 19. Comparison of transient membrane performance at 25 °C and 55 °C. Membrane: PTFE Schleicher & Schuell, 0.2 μm; P_{tm}: 0.3 bar; velocity: 1.3.

pores of membrane and thus the value of R_f decreases giving a higher permeate fluxrate. Details of the change of droplet size due to various conditions are discussed elsewhere [19].

5. Conclusions

The microfiltration of water in oil emulsions at ambient temperatures results in a fall in flux with time which is more significant in the initial stages of filtration. Analysis of the fall in flux with time for the PTFE and PVDF membranes indicates that cake formation gives the best prediction of behaviour. In the case of PVDF the model does not predict the performance over the complete range of filtration times but rather two-phases of filtration appear to occur; possibly cake formation initially followed by some intermediate pore blocking. In the case of the regenerated cellulose membrane, two stages of filtration seem to occur: which could be an initial phase of cake formation or some pore blocking followed by intermediate pore blocking.

An increase in temperature can significantly increase membrane performance. The steady state flux can increase by up to 43% with a temperature increase from 0 °C to 55 °C. This can be attributed to the increase in diffusivity and Reynolds Number with temperature, thus resulting in a significant increase in the mass transfer rate in the flow channel. The reduction in viscosity of the emulsion, due to an increase of temperature, also leads to a significant reduction in membrane fouling. Ideal non-fouling crossflow filtration can be achieved by operating at a temperature of 55 °C, crossflow velocity of 1.3 m s^{-1}, and at a transmembrane pressure of 0.3 bar.

Acknowledgements

Schleicher & Schuell and W M Gore supplied membranes for this research.

References

[1] R. Villarroel Lopez, S. Elmaleh, N. Ghaffor, Crossflow ultrafiltration of hydrocarbon emulsions, J. Membr. Sci. 102 (1995) 55–64.
[2] A.B. Koltuniewicz, R.W. Field, T.C. Arnot, Crossflow and dead-end nicrofiltration of oily-water emulsion. Part 1: Experimental study and analysis of flux decline, J. Membr. Sci. 102 (1995) 193–207.
[3] U. Daiminger, W. Nitsch, P. Plucinski, S. Hoffmann, Novel techniques for oil/water separation, J. Membr. Sci. 99 (1995) 197–203.
[4] A. Chinen, H. Ohya, Membrane microfiltration of oily water, Macromol. Symp. 118 (1997) 413–418.
[5] K. Scott, A. Adhamy, W. Atteck, C. Davidson, Crossflow microfiltration of organic/water suspensions, Water Res. 28 (1994) 137–145.
[6] A.B. Koltuniewicz, R.W. Field, Process factors during removal of oily-water emulsions with crossflow microfiltration, Desalination 105 (1996) 79–89.
[7] K. Scott, R.J.J. Jachuck, D. Hall, Crossflow microfiltration of water in oil emulsions using corrugated membranes, Sep. Purif. Technol. 22/23 (2001) 431–441.
[8] G.K. Anderson, C.B. Saw, M.S. Le, Oil/water separation with surface modified membranes, Environ. Technol. Lett. 8 (1987) 121–132.
[9] O. Le Barre, G. Daufin, Skim milk crossflow microfiltration performance versus permeation flux to wall shear, J. Membr. Sci. 117 (1996) 261–270.

[10] G.K. Dhawan, Emulsified oil waste water treatment by ultrafiltration, Ultrafiltr. Emulsif. Oily Wastes (1976) 189–199.
[11] J.T.F. Keurentjes, M.A. Cohen Stuart, D. Brinkman, C.G.P.H. Schroen, K. Uan't Riet, Surfactant induced wetting transitions: role of surface hydrophobicity and effect of oil permeability of ultrafiltration membranes, Colloid Surf. 51 (1990) 189–203.
[12] A. Van der Padt, J.J.W. Sewalt, K. Van't Riet, Specific byproduct removal in a membrane bioreactor, in: Proceedings of the Engineering of Membrane Processes Conference, 1992, p. 13.
[13] S.H. Lee, K.C. Chung, M.C. Shin, Preparation of ceramic membrane and application to the crossflow microfiltration of soluble waste oil, Mater. Lett. 4–5 (2002) 266–271.
[14] I. Limayem, C. Charcosset, H. Fessi, Purification of nanoparticle suspensions by a concentration/diafiltration process, Sep. Purif. Technol. 38 (2004) 1–9.
[15] S. Ripperger, J. Altmann, Crossflow microfiltration-state of the art, Sep. Purif. Technol. 26 (2002) 19–31.
[16] J. Hermia, Constant pressure blocking filtration law-application to power law non-Newtonian fluids, Trans. I Chem. E 60 (1982) 183–187.
[17] N.P. Cheremisinoff, Liquid Filtration, Elsevier, 1998.
[18] J. Murkes, C.G. Carlsson, Crossflow Filtr.: Theor. Pract. (1988).
[19] B. Hu, Crossflow microfiltration of water in oil emulsions. Ph.D. Thesis. University of Newcastle upon Tyne, 2001.